

## Caffeine-mediated synthesis of CuO nanoparticles: characterization, morphology changes, and bactericidal activity

A. P. Angeline Mary, A. Thaminum Ansari & R. Subramanian

To cite this article: A. P. Angeline Mary, A. Thaminum Ansari & R. Subramanian (2020): Caffeine-mediated synthesis of CuO nanoparticles: characterization, morphology changes, and bactericidal activity, *Inorganic and Nano-Metal Chemistry*, DOI: [10.1080/24701556.2020.1769667](https://doi.org/10.1080/24701556.2020.1769667)

To link to this article: <https://doi.org/10.1080/24701556.2020.1769667>



Published online: 25 May 2020.



Submit your article to this journal [↗](#)



Article views: 20



View related articles [↗](#)



View Crossmark data [↗](#)



# Caffeine-mediated synthesis of CuO nanoparticles: characterization, morphology changes, and bactericidal activity

A. P. Angeline Mary<sup>a</sup>, A. Thaminum Ansari<sup>b</sup>, and R. Subramanian<sup>c</sup>

<sup>a</sup>Department of Chemistry, Sacred Heart College, Tirupattur, Vellore, Tamil Nadu, India; <sup>b</sup>PG & Research Department of Chemistry, Muthurangam Government Arts College (Autonomous), Vellore, Tamil Nadu, India; <sup>c</sup>Department of Chemistry, Sun Arts and Science College, Tiruvannamalai, Tamil Nadu, India

## ABSTRACT

This study aims the synthesis of CuO nanoparticles using caffeine as stabilizing agent by precipitation method. The effect of caffeine on the morphology of CuO NPs was studied by varying the concentrations of caffeine. The synthesized CuO NPs were characterized using Fourier-transform infrared spectroscopy (FTIR), X-ray diffraction study (XRD) scanning electron microscopy coupled with energy-dispersive X-ray diffraction (SEM-EDAX), and transmission electron microscope with selected area diffraction (TEM-SAED). The morphological study of the nanoparticles shows that the leafy particles transformed into spherical nanoparticles at higher concentration of caffeine. The synthesized CuO NPs showed antibacterial activity against pathogenic bacteria. This research support to understand the role of caffeine in the synthesis of CuO NPs and further it could be used as material for biomedical applications.

## ARTICLE HISTORY

Received 21 February 2020  
Accepted 22 April 2020

## KEYWORDS

Caffeine; organic modifier; copper oxide; spherical nanoparticles

## Introduction

Nanomaterials such as metal and metal oxide nanoparticles attract the researchers around the world due to their peculiar properties and application.<sup>[1–4]</sup> Various properties and applications of nanomaterials make the researcher move toward green synthesis. Green synthesis of nanoparticles has attracted the researchers due to enormous applications. The numerous toxic effects of metal nanoparticles put effort to develop a green method to fabricate metal nanoparticles. Green fabrication of copper nanoparticles is of vast curiosity because of the many benefits. Environmental applications such as dye degradation, metal removal, and catalytic activities of nanoparticles also inspired for nanomaterial research.<sup>[1,5–9]</sup>

Copper is well known for its electrical conductivity than silver and gold.<sup>[10]</sup> Copper oxide nanoparticles are industrially important due to their physio-chemical properties. They used as superconductors, catalysis, batteries, and gas sensors. Its potentials also explored in the field of harvesting solar energy.<sup>[11]</sup> Copper oxide, a leading semi-conducting metal oxide, having a bandgap of 1.2 eV has inspired the attention of the researchers in industry and academia due to its tremendous applications.<sup>[12]</sup> The CuO NPs have been widely used for various applications such as solar cells, sensors, catalyst for dye degradations, and detecting biomolecules in the analysis.<sup>[13]</sup> The bioactive molecules present in the plant extract act as reducing agent for the synthesis of CuO NPs. Numerous plant extracts have been used as reducing agent to fabricate the CuO NPs. *Carica papaya* leaves,<sup>[14]</sup> Oak fruit



hull,<sup>[15]</sup> *Ixora coccinea* leaf,<sup>[16]</sup> *Syzygium alternifolium* (Wt.) Walp,<sup>[17]</sup> *Ferulago angulata* (Schlecht) Boiss,<sup>[18]</sup> *Rosa canina* fruit,<sup>[19]</sup> *Azadirachta indica*,<sup>[20]</sup> *Bauhinia tomentosa* leaves,<sup>[21]</sup> *Moringa oleifera* leaves,<sup>[22]</sup> wheat seed extract,<sup>[23]</sup> *Euphorbia chamaesyce* leaf extract<sup>[24]</sup> and many more plant extracts,<sup>[25]</sup> and *tragacanth* gel<sup>[26]</sup> have been used natural reducing in the green synthesis of CuO NPs.

Tea is a methylxanthine compound, rich source of caffeine. Caffeine activates the central nervous system (CNS). It is a psychoactive drug legally used around the world.<sup>[27]</sup> It reported to improve physical performance, memory, and cognitive performance. It increases energy, alertness, anxiety, and the capability to concentrate attention and reduces the fatigue.<sup>[28,29]</sup> Famous beverages such as black tea and coffee have been used to produce metal oxide nanoparticles Black tea.<sup>[3,30,31]</sup> It has many more health benefits. It is freely soluble in hot water. In the present work, we studied the effect of caffeine on crystalline structure, size, shape, and morphology of the copper nanoparticles.

## Experimental

### Chemicals

Copper nitrate and sodium hydroxide were procured from Loba Chemie, Mumbai, India. Distilled water was used as a solvent to prepare all the reagents. Caffeine was isolated from the tea dust using standard procedures and applied as a modifier.

\*CONTACT A. Thaminum Ansari  drthaminum@gmail.com  PG & Research Department of Chemistry, Muthurangam Government Arts College (Autonomous), Vellore-632002, Tamil Nadu, India.

### Isolation of caffeine

Caffeine was isolated according to the procedure cited in the literature.<sup>[32]</sup> Briefly, 100 g of tea dust was soaked in distilled water and boiled for 30 min and filtered. Dichloromethane was added to the tea filtrate, which taken into a separating funnel and shaken well. The organic layer was separated and evaporated to get the caffeine. The caffeine was used as stabilizing agent to synthesize CuO NPs.

### Synthesis of CuO NPs

CuO NPs were synthesized by precipitation method. Copper nitrate was used as a precursor and sodium hydroxide as hydrolyzing agent. In brief, the requisite amount of caffeine was dissolved in 0.1 M of the copper nitrate solution, which taken in a 250 ml conical flask and heated on magnetic stirrer at 80 °C for half an hour. Then, the sodium hydroxide solution was slowly added to the above reaction mixture and continuously stirred for 4 h. The precipitate formed was thoroughly washed with distilled water to remove untreated reactants and organic matter. The precipitate was dried in an oven at 100 °C for 3 h. The copper hydroxide was annealed at 500 °C in a muffle furnace for 3 h to obtain the copper oxide. The samples prepared using 50, 100, and 200 mg of caffeine with the same procedure were named as CF1, CF2, and CF3. A blank one prepared without caffeine was named as CF0.

### Characterization techniques

The X-ray diffraction studies were carried out using Cu-K $\alpha$  radiation (Model: X'Pert-PRO) instrument and scanned in the range of 10–80 °C of  $2\theta$  values. Functional group identification and formation of Cu-O bond were analyzed by Jasco 6300 FT-IR spectrophotometer in the frequency range from 500 to 4000  $\text{cm}^{-1}$ . Nucleation and Morphology of CuO NPs were examined by JEOL Model JSM-6390LV scanning electron microscope. The elemental composition was analyzed using energy-dispersive study (EDS). JEOL/JEM 2100 transmission electron microscope was used to analyze the shape and surface morphology of the nanoparticles. The state of the chemical state and elemental composition of the elements existence in CuO NPs was determined by X-ray photoelectron spectroscopy (XPS, Thermo Scientific K-Alpha) equipped with an Al K $\alpha$  X-ray source. XPS with Auger electron spectroscopy (AES) Module: Model/Supplier:PHI 5000 Versa Prob II, FEI Inc. was used to find out the electronic states of copper oxide nanoparticles.

### Bactericidal activity

The antibacterial activity of caffeine stabilized CuO NPs was examined according to the procedure cited in the literature.<sup>[20]</sup> About 28 g of Muller Hinton agar was dissolved in 1000 ml distilled water. The disks were prepared using Whatman filter paper no. 1 with 6 mm diameter. Bacterial culture broths were prepared by using a loop of each

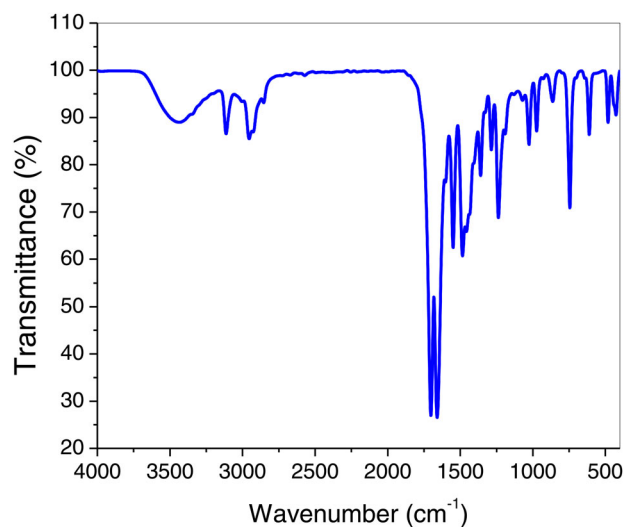


Figure 1. FTIR spectrum of caffeine.

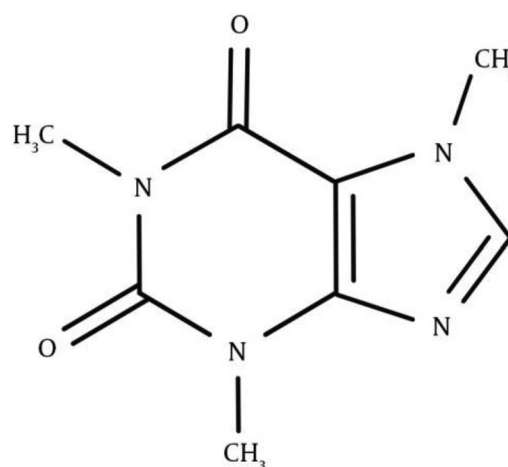
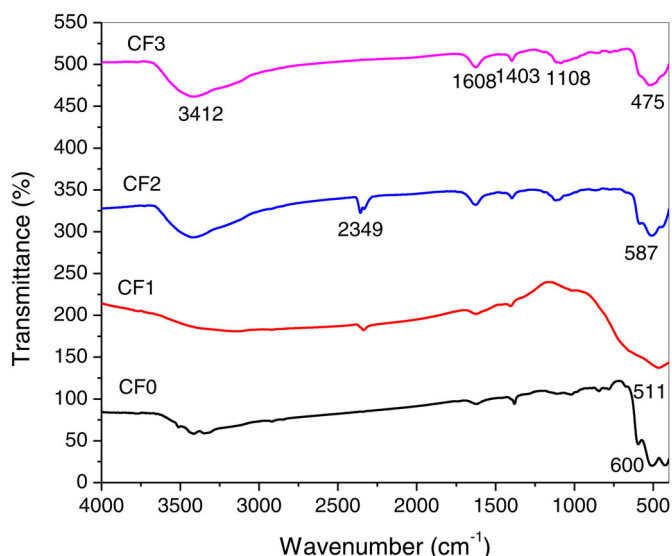


Figure 2. Structure of Caffeine.

bacterium and dispersed in 10 ml of Milli-Q water in each test tube. The bacterial suspension used to be  $10^6$  CFU mL by diluting with normal saline solution. The sterilized nutrient agar was poured in each Petri plate and was mixed softly. After solidification, the sterilized filter paper disks were wrapped up in test samples and positioned at delineates position on agar medium. The Petri plates were incubated at 37 °C for 24 h. The concentration of CuO NPs used was 100  $\mu\text{g}/\text{ml}$ . The zone of inhibition around the disks was determined and mentioned as mean  $\pm$  standard error of the mean.

### Results and discussion

An attempt has been made to study the effect of caffeine on the surface morphology, size, and shape of copper oxide nanoparticles. Caffeine is a natural substance was isolated from the tea dust used as stabilizing agent. The FTIR spectrum of caffeine was shown in Figure 1. The spectrum of caffeine show the absorbance band at 827, 921, 987, 1045, 1103, 1267, 1346, 1411, 1633, 2933, and 3263  $\text{cm}^{-1}$ . The structure of caffeine is shown in Figure 2 comprises of C-H,  $\text{CH}_3$ , C-N, C=O, and C-C bonds. The band at 827, 921,



**Figure 3.** FTIR spectra of CuO NPs synthesized using caffeine; CF0-CuO without caffeine; CF1-CF3-CuO NPs synthesized using 50, 100, and 200 mg caffeine.

987, and 1045  $\text{cm}^{-1}$  are attributed the stretching of C-C bonds of caffeine. The bands observed at 1103 and 1267  $\text{cm}^{-1}$  are attributed to the stretching vibrations of C=O and C-N bonds. The bands observed at 1346 and 1411  $\text{cm}^{-1}$  relevant to stretching vibrations of C-N and C=C of caffeine. A band noted at 1633  $\text{cm}^{-1}$  due to the stretching vibration of the carbonyl group (C=O). Two larger bands noticed at 2933 and 3263  $\text{cm}^{-1}$  are ascribed to the C-H bonds of methyl groups ( $\text{CH}_3$ ).<sup>[33]</sup>

The FTIR spectrum CuO NPs synthesized using caffeine is shown in Figure 3(a-d). The characteristic absorption bands at 521, 602, 773, 854, 1024, 1390, 1618, 3330, and 3140  $\text{cm}^{-1}$  observed in the FTIR spectra reveal the formation of CuO NPs. The band at 521 and 602  $\text{cm}^{-1}$  are due to stretching vibrations of Cu-O bond in CuO NPs. Two bands observed at 773 and 854  $\text{cm}^{-1}$  are attributed to the metal-oxygen, stretching vibrations of CuO NPs.<sup>[34]</sup> The bands observed at 1618 and 3410  $\text{cm}^{-1}$  are represented to stretching vibrations of moisture content on the surface of CuO NPs. The characteristic absorption bands observed at 522, 773, 842, 1093, 1401, 1629, and 3422  $\text{cm}^{-1}$  confirms the formation of CuO NPs.<sup>[35,36]</sup>

The XRD pattern of pure and CuO NPs synthesized using 50, 100, and 200 mg are shown in Figure 4(a-d). The given spectrum shows the crystalline nature of CuO NPs. The XRD pattern revealed a sequence of diffraction peaks at  $2\theta$  of X-axis at 32.45°, 35.69°, 38.71°, 48.08°, 53.56°, 58.32°, 61.68°, 66.58, 68.51°, 2.62°, and 75.65° coincide with (110), (002), (111), (202), (020), (202), and (113) planes, respectively. The diffraction peaks are matched with JCPDS Card (No. 89-2529), which evidently reveal the caffeine mediated synthesized CuO NPs are in mono-clinic structure.<sup>[37-39]</sup> The absence of extra peaks in the spectrum revealed that the CuO NPs are in pure phase. Crystallite size was calculated using the Scherrer Equation (1).

$$D = \frac{K\lambda}{\beta \cos\theta} \quad (1)$$

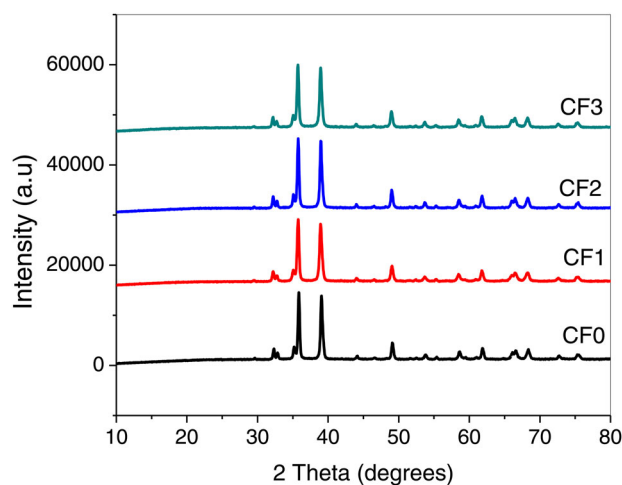


**Figure 4.** XRD pattern of CuO NPs (CF0) CuO NPs produced without caffeine (CF1-CF3) CuO NPs produced using 50, 100, and 200 mg caffeine.

where  $D$  is the mean size of the crystalline;  $K$  is a dimensionless shape factor, with a value close to unity (0.9).  $\lambda$  is the X-ray wavelength;  $\beta$  is the line broadening at half the maximum intensity (FWHM);  $\theta$  is the Bragg angle. The average crystallite size of the CF0, CF1, CF2, and CF3 calculated were found to be 125, 116, 123, and 138 nm, respectively.

Figure 5(a) shows the SEM images of CuO synthesized without caffeine. It shows leafy and irregular shaped micro-particles. Figure 5(b) shows the SEM images of CuO synthesized using 50 mg of caffeine. It obviously shows that the particles are leaf and arranged in such a way to form, which are free from agglomeration. Further, it is observed that microstructure is dependent concentration of caffeine. Figure 5(c,d) shows that the CuO NPs are leafy and irregular fiber-like particles. From the SEM images, CuO NPs synthesized using 50 mg of caffeine considered as good in shape when compared with CuO prepared with 100 and 200 mg of caffeine as well as blank one. As noticed in figure, the images reveal lengthy and leafy microparticles. The presence of Cu and O confirmed by EDS as shown in Figure 5(e). The morphology of nanoparticles synthesized using 100 and 200 mg appeared to be similar in morphology. But they differ from pure and CuO NPs synthesized using 50 mg of caffeine. The EDS investigation exposed the percentage of Cu and O in all the samples.

Figure 6(a-d) show the variation of the size of obtaining nanoparticles with various concentrations of caffeine. As seen in the images, with caffeine increasing, the size of nanoparticles found to be similar which varies from the SEM morphology. Reduction of nanoscale size is due to the interaction between caffeine and  $\text{Cu}^{2+}$  ions. A subsequent increase in size of the particles might be attributed to the fairly increasing growth rate of particles during the nucleation. The arrangement of particles seen in the SEM images further confirmed by the SAED pattern. Bright particles are observed in the SAED pattern of CuO NPs without caffeine reveal bigger size particles. The SAED pattern of CuO produced with 50 mg caffeine found to be a uniform pattern in the (Figure 6) The TEM study is performed to understand

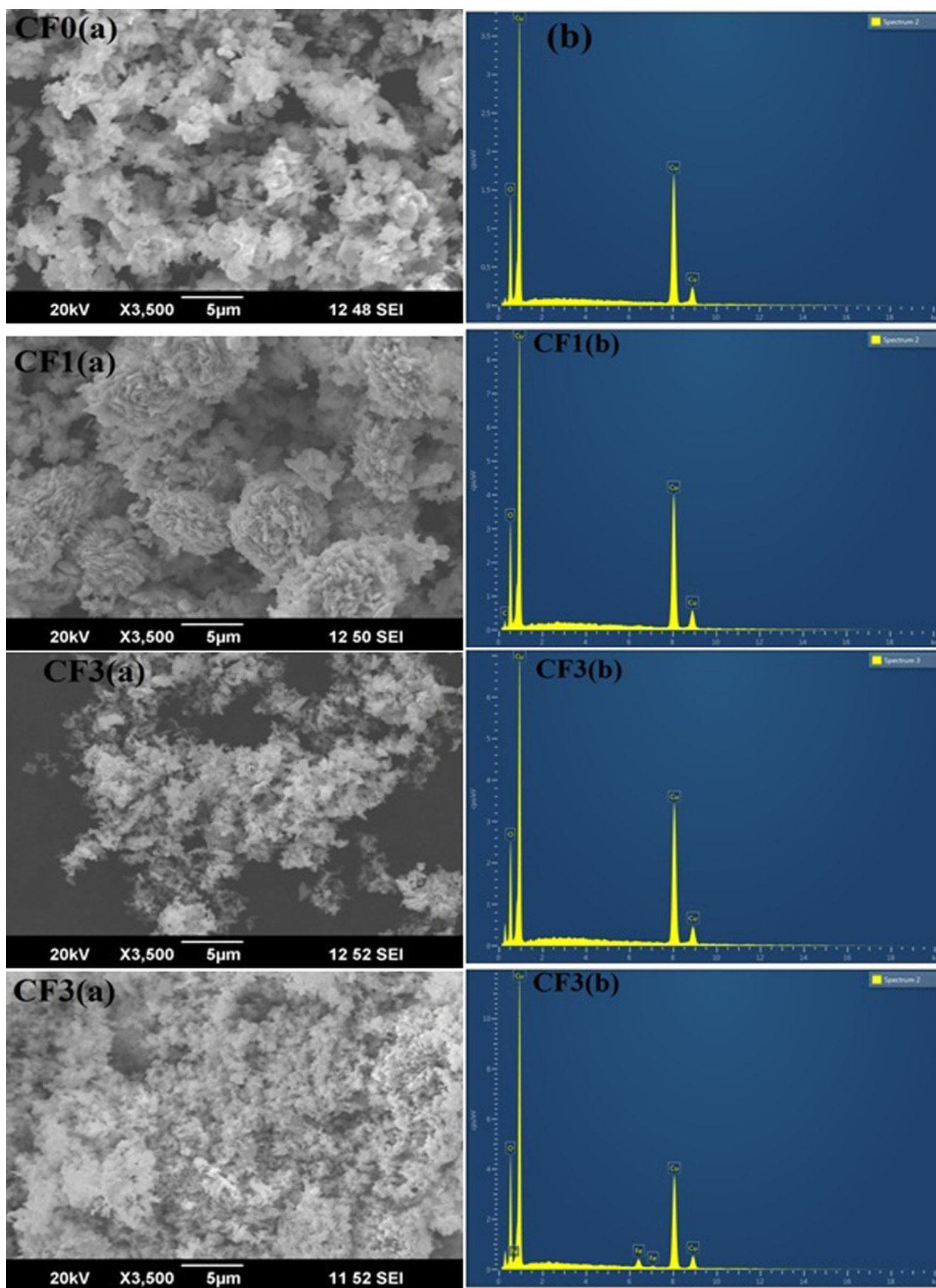
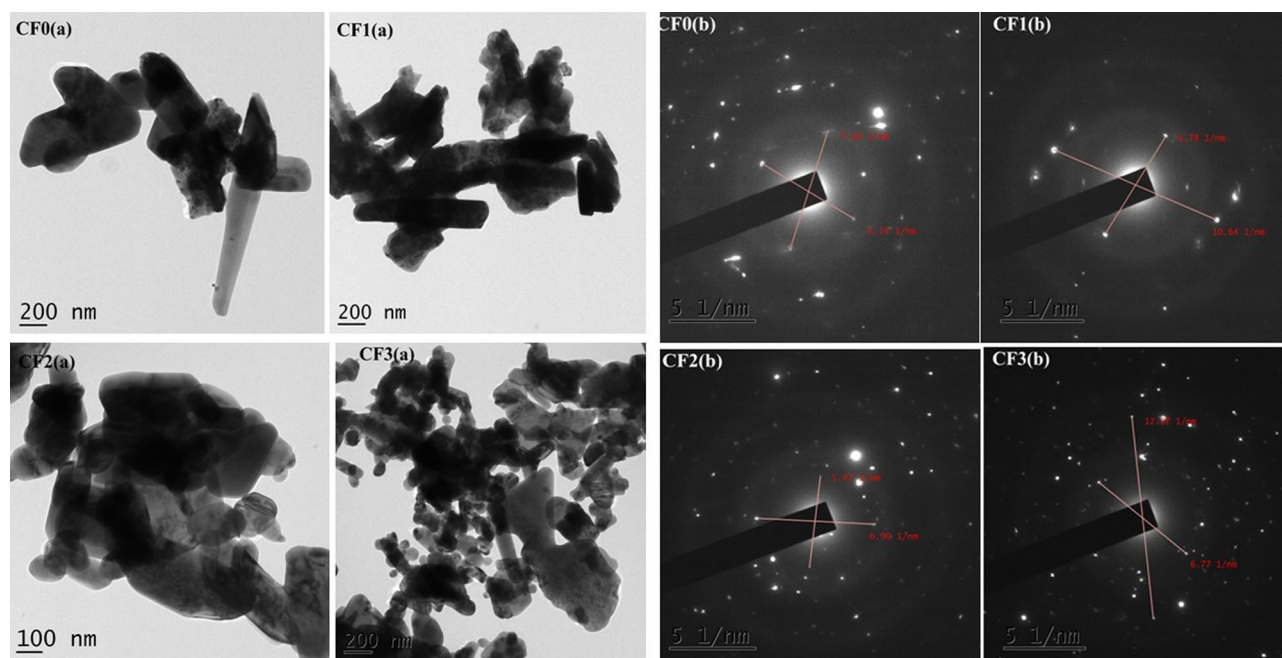
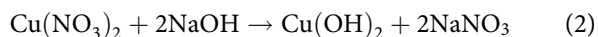


Figure 5. SEM photographs of CuO NPs; (CF0) CuO NPs produced without caffeine, (CF1-CF3) CuO NPs produced using 50, 100, and 200 mg caffeine.



**Figure 6.** (a) TEM morphographs of CuO NPs; (CF0) CuO NPs produced without caffeine (CF1-CF3) CuO NPs produced using 50, 100, and 200 mg caffeine. (b) Selected area diffraction pattern of CuO nanoparticles; CF0(b) SAED pattern of CuO synthesized without caffeine, CF1-CF3(b)-SAED pattern of CuO synthesized using 50, 100, and 200 mg caffeine.

the morphology, shape, size and the crystalline characteristics of the nanoparticles. The particles are observed to be spherical in shape and the size is found to be in the range of 10–50 nm. It is well known that sugarcane juice contains glucose and fructose as major components CuO NPs synthesized using caffeine. It has been proved that the caffeine can act as a surface modifier, stabilizing and capping agents, which control the morphology.<sup>[40,41]</sup> The formation mechanism of CuO NPs is given by Equations (2) and (3). Copper nitrate reacts with reducing agent (sodium hydroxide solution) to produce copper hydroxide. During the reaction, caffeine has interacted with react with the copper hydroxide and produce changes in surface morphology.



First, copper nitrate is converted into copper hydroxide when 0.1 M sodium hydroxide was used as a hydrolyzing agent in the presence of caffeine. It is assumed that the caffeine interacts with copper hydroxide to produce different shapes of nanoparticles. As the concentration of caffeine increased from 50 mg to 200 mg, nanorods transformed into spherical particles. The copper hydroxide colloids were stored in the laboratory, after three months, the particles totally settled down.

Further, the formation of CuO nanoparticles was confirmed by high-resolution XPS to study the electronic structure, oxidation state, and the composition of the atoms involved, and the results are shown in Figure 7(a–c). Three peaks were indexed to Cu, C, and O. The survey of the surface presents all the elements detected as shown in the figure represents binding energy peaks at 282.15, 526.98, and 931.16 eV which are attributed to C 1s, O 1s, and Cu 2p,

respectively. In Figure 7(c), the Cu 2p<sub>3/2</sub> is allocated at 931.22 eV with a shoulder peak at about 941.55 eV and Cu 2p<sub>1/2</sub> lies at 951.26 eV with a peak at about 959.94 eV due to the 3d<sup>9</sup> shell resultant for the Cu<sup>+</sup> state. The difference between the Cu 2p<sub>3/2</sub> and Cu 2p<sub>1/2</sub> is 20.09 eV, which is in concordance with the standard value of 20.10 eV for CuO. The XPS spectra of O 1s evidenced by two broad peaks that correspond to the O<sub>2</sub> in CuO NPs. The main peak appeared at the lower binding energy of 526.98 eV is attributed to Cu–O (Figure 7(b)). A broad peak at 282.15 eV (Figure 7(a)), lower binding energy attributed to C 1s may be due to the biomass content and an adsorbed carbon dioxide molecule on the surface of CuO.<sup>[42–44]</sup>

### Bactericidal activity

The bactericidal activity of ciprofloxacin (25 μg) and CuO NPs (100 μg) were tested in a Petri plate. The zone of inhibition exhibited by CuO against *Escherichia coli*, *Bacillus subtilis*, *Pseudomonas epidermidis*, and *Staphylococcus aureus*. The zone of inhibition shown by all the samples is presented in Table 1. Among the four samples, CF2 and CF3 showed maximum zone inhibition against tested bacteria. The obtained results are compared with standard antibiotic substance ciprofloxacin.

### Conclusions

This research work reports the synthesis of CuO NPs using caffeine as a stabilizing agent. FTIR and XRD pattern analysis confirmed the formation of CuO NPs and their crystalline nature. The SEM morphographs confirmed the formation of microparticles with various shapes. The TEM images revealed the transformation, shape, and size of the

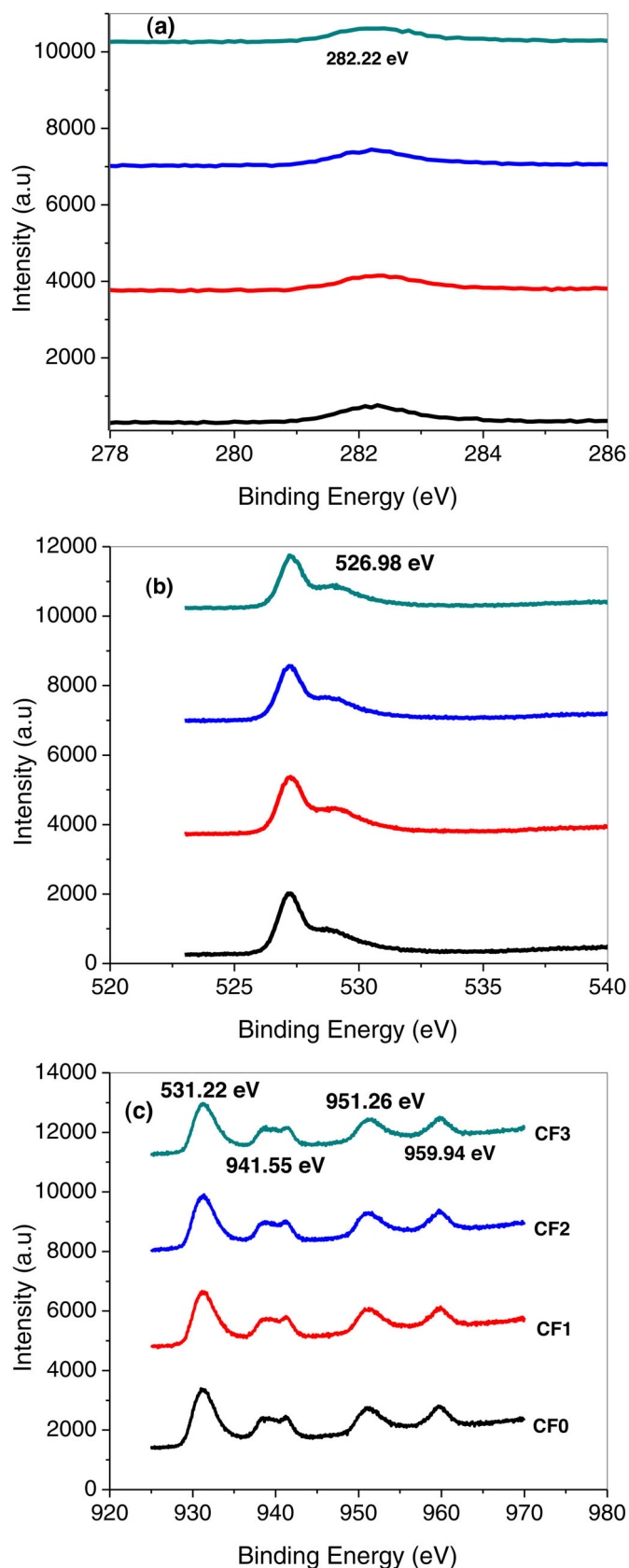


**Figure 7.** XPS analysis of caffeine stabilized CuO NPs: (CF0) CuO NPs without caffeine; (CF1–CF3) CuO NPs stabilized with 50, 100, and 200 mg caffeine; (a) C 1s (b) O 1s (c) Cu 2p.

particles from irregular to spherical. The size and shape of the particles found to be reduced at higher concentration of caffeine. In addition, the above mentioned various shapes of

**Table 1.** Average zone of inhibition for various concentrations of CuO NPs nanoparticles in (mm).

Microorganisms	CF0	CF1	CF2	CF3	Ciprofloxacin (25 µg)
<i>E. coli</i>	10	11	12	16	23
<i>B. subtilis</i>	8	7	14	12	19
<i>S. epidermidis</i>	10	11	8	10	18
<i>S. aureus</i>	12	9	12	12	17

particles disappeared at higher concentrations and produced spherical-shaped particles. This work proved that the sugarcane is a suitable green stabilizing agent to produce copper oxide nanoparticles. CuO NPs exhibited significant bactericidal activity against *E. coli*, *S. aureus*, *Pseudomonas aeruginosa*, and *B. subtilis*. Synthesis of copper oxide nanoparticles suggests that the caffeine acts as a surface modifier and stabilizing agent.

### Acknowledgments

The authors gratefully acknowledge the authority of STIC, CUSAT, Cochin for providing the SEM and TEM images for this study. The authors thank the Director, IIT Indore for providing XPS analysis.

### Disclosure statement

The authors declare that they have no conflict of interest.

### References

- Moradnia, F.; Fardood, S. T.; Ramazani, A.; Vinod Kumar, G. Green Synthesis of Recyclable MgFeCrO<sub>4</sub> Spinel Nanoparticles for Rapid Photodegradation of Direct Black 122 Dye. *J. Photoch. Photobio. A* **2020**, *392*, 112433. DOI: [10.1016/j.jphotochem.2020.112433](https://doi.org/10.1016/j.jphotochem.2020.112433).
- Fardood, S. T.; Ramazani, A.; Moradnia, F.; Afshari, Z.; Ganjkanlu, S.; Yekke Zare, F. Green Synthesis of ZnO Nanoparticles via Sol-Gel Method and Investigation of Its Application in Solvent-Free Synthesis of 12-Aryl-Tetrahydrobenzo[*a*]Xanthene-11-One Derivatives under Microwave Irradiation. *Chem. Method* **2019**, *3*, 696–706.
- Fardood, S. T.; Ramazani, A.; Joo, S. W. Sol-Gel Synthesis and Characterization of Zinc Oxide Nanoparticles Using Black Tea Extract. *J. Appl. Chem. Res.* **2017**, *11*, 8–17.
- Ramazani, A.; Fardood, S. T.; Hosseinzadeh, Z.; Sadri, F.; Joo, S. W. Green Synthesis of Magnetic Copper Ferrite Nanoparticles Using Tragacanth Gum as a Biotemplate and Their Catalytic Activity for the Oxidation of Alcohols. *Iran. J. Catal.* **2017**, *7*, 181–185.
- Atrak, K.; Ramazani, A.; Fardood, S. T. Green Synthesis of Amorphous and Gamma Aluminum Oxide Nanoparticles by Tragacanth Gel and Comparison of Their Photocatalytic Activity for the Degradation of Organic Dyes. *J. Mater. Sci. Mater. Electron.* **2018**, *29*, 8347–8353. DOI: [10.1007/s10854-018-8845-2](https://doi.org/10.1007/s10854-018-8845-2).
- Fardood, S. T.; Forootan, R.; Moradnia, F.; Afshari, Z.; Ramazani, A. Green Synthesis, Characterization, and Photocatalytic Activity of Cobalt Chromite Spinel Nanoparticles. *Mater. Res. Express.* **2020**, *7*, 015086. DOI: [10.1088/2053-1591/ab6c8d](https://doi.org/10.1088/2053-1591/ab6c8d).
- Moradnia, F.; Ramazani, A.; Fardood, S. T.; Gouranlou, F. A Novel Green Synthesis and Characterization of Tetragonal-Spinel MgMn<sub>2</sub>O<sub>4</sub> Nanoparticles by *Tragacanth* Gel and Studies of its Photocatalytic Activity for Degradation of Reactive Blue 21 Dye under Visible Light. *Mater. Res. Express.* **2019**, *6*, 075057. DOI: [10.1088/2053-1591/ab17bc](https://doi.org/10.1088/2053-1591/ab17bc).

8. Yeganeh, M. S.; Reza Kazemizadeh, A.; Ramazani, A.; Eskandari, P.; Angourani, H. R. Plant-Mediated Synthesis of  $\text{Cu}_{0.5}\text{Zn}_{0.5}\text{Fe}_2\text{O}_4$  Nanoparticles Using *Minidium leavigatum* and Their Applications as an Adsorbent for Removal of Reactive Blue 222 Dye. *Mater. Res. Express.* **2020**, *6*, 1250f4. DOI: [10.1088/2053-1591/ab6637](https://doi.org/10.1088/2053-1591/ab6637).
9. Fardood, S. T.; Moradnia, F.; Mostafaei, M.; Afshari, Z.; Faramarzi, V.; Ganjkanlu, S. Biosynthesis of  $\text{MgFe}_2\text{O}_4$  Magnetic Nanoparticles and Their Application in Photodegradation of Malachite Green Dye and Kinetic Study. *Nanochem. Res.* **2019**, *4*, 86–93.
10. Suresh, Y.; Annapurna, S.; Singh, A. K.; Bhikshamaiah, G. Green Synthesis and Characterization of Tea Decoction Stabilized Copper Nanoparticles. *Int. J. Innov. Res.Sci. Eng. Technol.* **2014**, *3*, 11265–11270.
11. Peternela, J.; Silva, M. F.; Vieira, M. F.; Bergamasco, R.; Salcedo Vieira, A. M. Synthesis and Impregnation of Copper Oxide Nanoparticles on Activated Carbon Through Green Synthesis for Water Pollutant Removal. *Mater. Res.* **2018**, *21*, e20160460.
12. Chen, H.; Zhao, G.; Liu, Y. Low-Temperature Solution Synthesis of  $\text{CuO}$  Nanorods with Thin Diameter. *Mater. Lett.* **2013**, *93*, 60–63. DOI: [10.1016/j.matlet.2012.11.055](https://doi.org/10.1016/j.matlet.2012.11.055).
13. Chang, Y. N.; Zhang, M.; Xia, L.; Zhang, J.; Xing, G. The Toxic Effects and Mechanisms of  $\text{CuO}$  and  $\text{ZnO}$  Nanoparticles. *Materials* **2012**, *5*, 2850–2871. DOI: [10.3390/ma5122850](https://doi.org/10.3390/ma5122850).
14. Sankar, R.; Manikandan, P.; Malarvizhi, V.; Fathima, T.; Shivashangari, K. S.; Ravikumar, V. Green Synthesis of Colloidal Copper Oxide Nanoparticles Using Carica Papaya and Its Application in Photocatalytic Dye Degradation. *Spectrochim. Acta Part A Mol. Biomol. Spectrosc.* **2014**, *121*, 746–750. DOI: [10.1016/j.saa.2013.12.020](https://doi.org/10.1016/j.saa.2013.12.020).
15. Sorbiun, M.; Shayegan, E.; Ali, M. Green Synthesis of Zinc Oxide and Copper Oxide Nanoparticles Using Aqueous Extract of Oak Fruit Hull (Jaft) and Comparing Their Photocatalytic Degradation Of Basic Violet 3. *Int. J. Environ. Res.* **2018**, *12*, 29–37.
16. Vishveshvar, K.; Krishnan, M. V. A.; Haribabu, K.; Vishnuprasad, S. Green Synthesis of Copper Oxide Nanoparticles Using *Ixiro coccinea* Plant Leaves and Its Characterization. *BioNanoSci.* **2018**, *8*, 554–537. DOI: [10.1007/s12668-018-0508-5](https://doi.org/10.1007/s12668-018-0508-5).
17. Yugandhar, P.; Vasavi, T.; Jayavardhana Rao, Y.; Uma Maheswari Devi, P.; Narasimha, G.; Savithramma, N. Cost Effective, Green Synthesis of Copper Oxide Nanoparticles Using Fruit Extract of *Syzygium alternifolium* (Wt.) Walp., Characterization and Evaluation of Antiviral Activity. *J. Clust. Sci.* **2018**, *29*, 743–755. DOI: [10.1007/s10876-018-1395-1](https://doi.org/10.1007/s10876-018-1395-1).
18. Shayegan, E.; Mina, M.; Ali, S.; Saeid, R.; Fardood, T. Plant-Mediated Synthesis of Zinc Oxide and Copper Oxide Nanoparticles by Using *Ferulago angulata* (schlecht) Boiss Extract and Comparison of Their Photocatalytic Degradation of Rhodamine B (RhB) under Visible Light Irradiation. *J. Mater. Sci. Mater. Electron.* **2018**, *29*, 1333–1340.
19. Hemmati, S.; Mehrazin, L.; Hekmati, M.; Izadi, M.; Veisi, H. Biosynthesis of  $\text{CuO}$  Nanoparticles Using *Rosa canina* Fruit Extract as a Recyclable and Heterogeneous Nanocatalyst for C-N Ullmann Coupling Reactions. *Mater. Chem. Phys.* **2018**, *214*, 527–532. DOI: [10.1016/j.matchemphys.2018.04.114](https://doi.org/10.1016/j.matchemphys.2018.04.114).
20. Sharma, B. L.; Shah, D. V.; Roy, D. R. Green Synthesis of  $\text{CuO}$  Nanoparticles Using *Azadirachta indica* and Its Antibacterial Activity for Medicinal Applications. *Mater. Res. Express.* **2018**, *5*, 095033. doi:MRX-109160.R1 DOI: [10.1088/2053-1591/aad91d](https://doi.org/10.1088/2053-1591/aad91d).
21. Sharmila, G.; Sakthi Pradeep, R.; Sandiy, K.; Santhiya, S.; Muthukumaran, C.; Jeyanthi, J.; Manoj Kumar, N.; Thirumarimurugan, M. Biogenic Synthesis of  $\text{CuO}$  Nanoparticles Using *Bauhinia tomentosa* Leaves Extract: Characterization and Its Antibacterial Application. *J. Mol. Struct.* **2018**, *1165*, 288–292. DOI: [10.1016/j.molstruc.2018.04.011](https://doi.org/10.1016/j.molstruc.2018.04.011).
22. Galan, C. R.; Silva, M. F.; Mantovani, D.; Bergamasco, R.; Vieira, M. F. Green Synthesis of Copper Oxide Nanoparticles Impregnated on Activated Carbon Using *Moringa oleifera* Leaves Extract for the Removal of Nitrates from Water. *Can. J. Chem. Eng.* **2018**, *96*, 2378–2379. DOI: [10.1002/cjce.23185](https://doi.org/10.1002/cjce.23185).
23. Buazar, F.; Sweidi, S.; Badri, M.; Kroushawi, F. Biofabrication of Highly Pure Copper Oxide Nanoparticles Using Wheat Seed Extract and Their Catalytic Activity: A Mechanistic Approach. *Green Process Synth.* **2019**, *8*, 691–702. DOI: [10.1515/gps-2019-0040](https://doi.org/10.1515/gps-2019-0040).
24. Maham, M.; Sajadi, S. M.; Kharimkhani, M. M.; Nasrollahzadeh, M. Biosynthesis of the  $\text{CuO}$  Nanoparticles Using *Euphorbia chamaesyce* Leaf Extract and Investigation of Their Catalytic Activity for the Reduction of 4-Nitrophenol. *IET Nanobiotechnol.* **2017**, *11*, 766–772. DOI: [10.1049/iet-nbt.2016.0254](https://doi.org/10.1049/iet-nbt.2016.0254).
25. Ananda Murthy, H. C.; Abebe, B.; C H, P.; Shantaveerayya, K. A Review on Green Synthesis and Applications of  $\text{Cu}$  and  $\text{CuO}$  Nanoparticles. *Mat. Sci. Res. India* **2018**, *15*, 279–295. DOI: [10.13005/msri/150311](https://doi.org/10.13005/msri/150311).
26. Fardood, S. T. ;A.; Ramazani, A.; Joo, S. W. Green Chemistry Approach for the Synthesis of Copper Oxide Nanoparticles Using *Tragacanth* Gel and Their Structural Characterization. *J. Struct. Chem.* **2018**, *59*, 482–486. DOI: [10.1134/S0022476618020324](https://doi.org/10.1134/S0022476618020324).
27. Nehlig, A.; Daval, J. L.; Debry, G. Caffeine and the Central Nervous System: Mechanisms of Action, Biochemical, Metabolic and Psycho Stimulant Effects. *Brain Res. Brain Res. Rev.* **1992**, *17*, 139–170. DOI: [10.1016/0165-0173\(92\)90012-B](https://doi.org/10.1016/0165-0173(92)90012-B).
28. Glade, M. J. Caffeine-Not Just a Stimulant. *Nutrition* **2010**, *26*, 932–938. DOI: [10.1016/j.nut.2010.08.004](https://doi.org/10.1016/j.nut.2010.08.004).
29. Baratloo, A.; Rouhipour, A.; Forouzanfar, M. M.; Safari, S.; Amiri, M.; Negida, A. The Role of Caffeine in Pain Management: A Brief Literature Review. *Anesth. Pain Med.* **2016**, *6*, e33193. DOI: [10.5812/aapm.33193](https://doi.org/10.5812/aapm.33193).
30. Fardood, S. T.; Ramazani, A. Green Synthesis and Characterization of Copper Oxide Nanoparticles Using Coffee Powder Extract. *J. Nanostruct.* **2016**, *6*, 167–171.
31. Fardood, S. T.; Ramazani, A. Black Tea Extract Mediated Green Synthesis of Copper Oxide Nanoparticles. *J. Appl. Chem. Res.* **2018**, *12*, 8–15.
32. Subramanian, R.; Murugan, P.; Chinnadurai, G.; Ponnurugan, K.; Al-Dhabi, N. A. Experimental Studies on Caffeine Mediated Synthesis of Hydroxyapatite Nanorods and Their Characterization. *Mater. Res. Express.* **2020**, *7*, 015022. DOI: [10.1088/2053-1591/ab619a](https://doi.org/10.1088/2053-1591/ab619a).
33. Elango, M.; Deepa, M.; Subramanian, R.; Saraswathy, G. Effect of Piperine on Size, Shape and Morphology of Hydroxyapatite Nanoparticles Synthesized by the Chemical Precipitation Method. *Mater. Chem. Phys.* **2018**, *216*, 305–315. DOI: [10.1016/j.matchemphys.2018.05.049](https://doi.org/10.1016/j.matchemphys.2018.05.049).
34. Paradkar, M. M.; Irudayaraj, J. A Rapid FTIR Spectroscopic Method for Estimation of Caffeine in Soft Drinks and Total Methylxanthines in Tea and Coffee. *J. Food Sci.* **2002**, *67*, 2507–2511. DOI: [10.1111/j.1365-2621.2002.tb08767.x](https://doi.org/10.1111/j.1365-2621.2002.tb08767.x).
35. Prakash, S.; Elavarasan, N.; Venkatesan, A.; Subashini, K.; Sowndharya, M.; Sujatha, V. Green Synthesis of Copper Oxide Nanoparticles and Its Effective Applications in Biginelli Reaction, BTB Photodegradation and Antibacterial Activity. *Adv. Powder Tech.* **2018**, *29*, 3315–3326. DOI: [10.1016/j.apt.2018.09.009](https://doi.org/10.1016/j.apt.2018.09.009).
36. Thekkae Padil, V. V.; Černík, M. Green Synthesis of Copper Oxide Nanoparticles Using Gum Karaya as a Biotemplate and Their Antibacterial Application. *Int. J. Nanomed* **2013**, *8*, 889–898.
37. Liu, P.; Li, Z.; Cai, W.; Fang, M.; Luo, X. Fabrication of Cuprous Oxide Nanoparticles by Laser Ablation in PVP Aqueous Solution. *RSC Adv.* **2011**, *1*, 847–851. DOI: [10.1039/c1ra00261a](https://doi.org/10.1039/c1ra00261a).
38. Kuppasamy, P.; Ilavenil, S.; Srigopalram, S.; Maniam, G. P.; Yusoff, M. M.; Govindan, N.; Choi, K. C. Treating of Palm Oil Mill Effluent Using *Commelina nudiflora* Mediated Copper Nanoparticles as a Novel Bio-Control Agent. *J. Clean. Prod.* **2017**, *141*, 1023–1029. DOI: [10.1016/j.jclepro.2016.09.176](https://doi.org/10.1016/j.jclepro.2016.09.176).



39. Bhattacharjee, A.; Ahmaruzzaman, M. CuO Nanostructures: Facile Synthesis and Applications for Enhanced Photodegradation of Organic Compounds and Reduction of *p*-Nitrophenol from Aqueous Phase. *RSC Adv.* **2016**, *6*, 41348–41363. DOI: [10.1039/C6RA03624D](https://doi.org/10.1039/C6RA03624D).
40. Angeline Mary, A. P.; Thaminum Ansari, A.; Subramanian, R. Sugarcane Juice Mediated Synthesis of Copper Oxide Nanoparticles, Characterization and Their Antibacterial Activity. *J. King Saud Uni. Sci.* **2019**, *31*, 1103–1114. DOI: [10.1016/j.jksus.2019.03.003](https://doi.org/10.1016/j.jksus.2019.03.003).
41. Subramanian, R.; Sathish, S.; Murugan, P.; Mohamed Musthafa, A.; Elango, M. Effect of Piperine on Size, Shape and Morphology of Hydroxyapatite Nanoparticles Synthesized by the Chemical Precipitation Method. *J. King Saud Uni. Sci.* **2019**, *31*, 667–673. DOI: [10.1016/j.jksus.2018.01.002](https://doi.org/10.1016/j.jksus.2018.01.002).
42. Nagajyothi, P. C.; Muthuraman, P.; Sreekanth, T. V. M.; Hwan Kim, D.; Shim, J. Green Synthesis: In-Vitro Anticancer Activity of Copper Oxide Nanoparticles against Human Cervical Carcinoma Cells. *Arab. J. Chem.* **2017**, *10*, 215–225. DOI: [10.1016/j.arabjc.2016.01.011](https://doi.org/10.1016/j.arabjc.2016.01.011).
43. Sasikala, S.; Ganesh, V.; Seong, J. K. Biosynthesis of Copper Oxide (CuO) Nanowires and Their Use for the Electrochemical Sensing of Dopamine. *Nanomaterials* **2018**, *8*, 823.
44. Munawar, K.; Mansoor, M. A.; Basirun, W. J.; Misran, M.; Huang, N. M.; Mazhar, M. Single Step Fabrication of CuO–MnO–2TiO<sub>2</sub> Composite Thin Films with Improved Photoelectrochemical Response. *RSC Adv.* **2017**, *7*, 15885–15893. DOI: [10.1039/C6RA28752B](https://doi.org/10.1039/C6RA28752B).